

This equation is valid for $J \leq J_c$. For very small bias currents, the resistance is defined by the expression

$$R/R_{\max} = a \exp[-2(b/\tau)^{1/2}], \quad (17)$$

where $\tau = (T - T_{KT}) / (T_{c0} - T)$, a and b are constants, and R_{\max} is the resistance at temperatures above T_{c0} .

Kadin *et al.*⁴⁶ propose the following microscopic mechanism of formation of V-AV pairs as a result of photon absorption. A photon with energy $h\nu \gg 2\Delta$ is absorbed in a certain region (spot) at the surface of a 2D film, giving rise to a pair of highly excited quasiparticles which break additional Cooper pairs over a time period of the order of a few microseconds and distribute the excess energy among a large number of quasiparticles. These quasiparticles diffuse into the film over a depth $\sim \xi$ over a time $\sim h/k_B T_{KT}$ and suppress the order parameter Δ in this layer, as well as the critical current I_c . If the value of I_c in the region of the spot is smaller than the transport current I , this will lead to instability and a local collapse of Δ , causing the screening current to bend around this "hot spot." This process is analogous to phase slip induced by the phonon absorption, which provides the additional energy required by the current for the formation of a vortex pair (see Fig. 4). As a result of further diffusion of nonequilibrium quasiparticles into the film, the hot spot vanishes. However, the vortices continue to move at right angles to the current until they reach the edge of the film, leading to the emergence of a magnetic flux Φ_0 through the film which is equivalent to an integral voltage pulse. The time-averaged responsivity is given by $R_v = 1/(2e\nu)$.

The model described above, which was proposed for a homogeneous (on the scale $\sim \xi$) two-dimensional superconductor, can also be used for describing a 2D chain of weakly coupled JJ. It should be recalled that the effective field penetration depth λ_{eff} corresponding to weak intergranular currents may be quite large. Intergranular vortices with a reduced nucleation energy, and hence with a reduced pair dissociation energy, may emerge in such films. This explains the observed transition to vortex depairing in ordered chains of junctions as well as in granular superconductors. As soon as a vortex pair is formed, it behaves essentially in the same way as in a homogeneous film. For a granular superconductor with granule size $\leq \xi$, a photon absorbed in one of the granules suppresses Δ over the entire film, and reduces the critical currents linking it with the adjoining granules. This causes a local deviation of the current (Fig. 4a) followed by the formation of a vortex pair (Fig. 4b). In superconductors with a large size of the granules, however, a photon absorbed at the center of a granule hardly affects the intergranular currents. If the coupling between granules is not quite uniform, the vortex pairs formed in such granules cannot be dissociated by the current passing through them. In both these cases, the quantum efficiency of the process will be considerably reduced, which explains the large spread in the experimentally observed values of responsivity for granular thin-film HTSC detectors.

In spite of the fact that the formation of vortex pairs in this model occurs due to local heating, it was observed⁴⁹ that this is a nonequilibrium process and hence does not suffer from the drawbacks of bolometric detection. In this case, the

total heating of the film is quite insignificant while the local heating may be quite strong. Kadin *et al.*⁴⁹ proposed two possible regimes of formation of vortex pairs. For $h\nu < \Delta$, the absorption of a quantum is linked directly with the formation of a vortex pair. Such a pair is formed in two cases: (1) if the energy of the quantum at a given temperature is higher than the nucleation energy E_{v0} , and (2) if the total current $I_{\Sigma} = I + I_{\omega}$ (I is the bias current and I_{ω} the ac amplitude) exceeds the critical current I_c over a time long enough for the formation of a vortex. For $h\nu > \Delta$, Cooper pairs are dissociated at first. This is followed by the formation of a vortex pair as a result of local heating.

The response time in this model is determined by the fluxon velocity $v = J\Phi_0 / \eta = J\rho_n 2\pi\xi^2 / \Phi_0$ in a direction perpendicular to the applied current, where η is the viscosity of vortices in the Bardeen–Stefan theory, and ρ_n is the resistivity in the normal state. For $J \sim J_c$, since $J_c \rho_n \approx \Delta / e\xi$, we obtain the velocity $v \approx \Delta\xi / h$ which approaches the Fermi velocity $v_F = 10^7 - 10^8$ cm/s for a pure superconductor. For a film of width $w = 10 \mu\text{m}$ and $v_F = 10^7$ cm/s, we obtain the response time $t_R = 100$ ps. For sensitivity optimization, the working temperature must be lower than T_{KT} since the sensitivity at higher temperatures will be limited by the background voltage associated with thermally activated unpaired vortices and the magnetic field induced by the current.⁴⁹ The most suitable material for a detector is a film with uniformly linked small granules, for which the injection of vortices from the film edges is restricted. The absorption of a photon in HTSC leads to the formation of a vortex ring (three-dimensional analog of a 2D vortex pair) which is enlarged by the transport current and splits into a V-AV pair upon reaching the (lower and upper) film surface, leading to the same responsivity $R_v = \Phi_0 / h\nu$. In the one-dimensional case of a long wire with cross-sectional size $\sim \xi$, the absorption of a photon leads to the formation of a PSC which produces voltage steps.⁴⁶ For the one-dimensional case, the photon absorption may be accompanied by the formation of more than one PSC, which leads to an enhanced sensitivity below the quantum limit. In all other cases, the sensitivity of a film displaced in the vicinity of J_c is confined by the quantum limit since the violation of superconductivity due to the absorption of a photon is always connected with some kind of phase slip or a vortex process for which the magnetic flux quantum is a characteristic quantity.

Johnson *et al.*⁵⁰ studied the response of 10 nm-thick granular NbN films (with a grain size of the order of the film thickness) on Si substrates to optical radiation of wavelength $\Lambda = 632$ and 670 nm with a modulation frequency < 3.7 kHz and > 100 kHz, respectively. Meander-shaped structures with a constant surface area of 10^{-4} cm^2 ($5 \times 200 \mu\text{m}$, $10 \times 100 \mu\text{m}$, etc.) were prepared from these films. Below T_c , the authors⁵⁰ observed a slow bolometric response associated with film heating together with the substrate. It was found that radiation with wavelength $\leq 1 \mu\text{m}$ is absorbed strongly by Si and produces charge carriers in it. If the NbN film is displaced towards higher differential resistance, the conducting Si substrate partially shunts the response of the superconductor. In this case, the response becomes negative, i.e., the response amplitude decreases with increasing radiation

power. While the total response to continuous irradiation is positive, an increase in the modulation frequency transforms a slow positive signal into a fast negative signal. For high modulation frequencies, the slow bolometric response cannot “catch up” with the negative shunting component, and the net response is negative. In the absence of a bias current, when the laser beam is centered in the meander region, a rapid response which does not depend on the modulation frequency f_{mod} was observed up to 100 kHz. The authors associate this response with the photoelectric effect at the interface between NbN and Si. The photoelectric effect was not observed during optimization of the rapid positive component through an appropriate choice of the position of the laser beam.

The authors studied the transient and steady-state response as a function of the bias current I_b and temperature for $I_b < I_c$ and $T < T_c$. It was found that the dependences of the response δV_{ac} on $(\delta V / \delta T)_I$ are considerably nonlinear, especially in a constant weak magnetic field (up to 100 Oe). The nonlinear part of the dependence was observed for I_b corresponding to the highest differential resistance, and hence the shunting effect of the substrate was very strong. Measurement of $(\delta V / \delta T)_{I_b}$ for small I_b were used by the authors to estimate the effective sample heating $\delta T_{\text{eff}} \sim 150$ mK. The highest responsivity R_v was observed in currents close to I_b and was 125 V/W. Under the assumption that the positive response is associated only with the bolometric effect, the effective heating is theoretically estimated at 1–11 mK, which is much smaller than the experimental value. It is assumed that the observed response may be caused by two nonequilibrium mechanisms, i.e., either by electron heating effect, or by the kinetic inductivity mechanism. The former gives an extremely low value of $\delta T_{\text{eff}} \sim 1$ mK, as well as an underestimated value of responsivity. The authors believe that the photofluxon model of vortex-pair formation may explain the observed response, although the value of responsivity $R_v \sim 10^4$ V/W predicted by this model is much higher than the experimental value of 125 V/W. To prevent the excitation of photocarriers in Si and to avoid shunting of the response by the substrate, the same authors used a longer wavelength radiation source, viz., a diode laser with $\lambda = 1300$ nm, in their later work⁹ for a clearer differentiation of the response mechanisms. In the absence of a bias current, the responsivity of the response at radiation wavelengths 670 and 1300 nm was ~ 20 V/W. When the laser beam was centered on the meander, a positive response was observed. This response persisted as the frequency f_{mod} was increased to 1 MHz, and was attributed by the authors to the heating of the NbN film relative to the substrate. The response amplitude varied linearly with the radiation intensity, and the modulated response signal remained purely sinusoidal without any harmonics. The responsivity for rapid response was estimated at ~ 1500 V/W. The maximum possible heating of the sample did not exceed 2 mK.

Measurements of the dependence of the response on bias current and IVC at various temperatures led to the resistance $R_{\text{eff}}^{(T)}$ of the thermal boundary between the film and the sub-

strate. It was found that $R_{\text{eff}}^{(T)}$ depends strongly on I_b , while for a purely thermal effect it should not depend on current, but must have a significant temperature dependence. A comparison of the experimental results with the hot spot model⁵¹ reveals a good agreement for the temperature dependence of $R_{\text{eff}}^{(T)}$ near the transition, while the value of $R_{\text{eff}}^{(T)}$ obtained from the model for a deep superconducting state is found to be too low. It is borne out by computations⁹ that the thermal resistance $R_{\text{eph}}^{(T)}$ associated with a finite time τ_{eph} of energy transfer from electrons to phonons in the film makes a decisive contribution to the time characteristics of the response as compared with the Kapitza thermal resistance R_K due to a finite time of energy transfer from the phonons in the film to the phonons in the substrate.

Since the thermal conductivity estimates used in the model include the electron heating effect, and the quantity $(\partial V / \partial T)_{I_b}$ (which is also used in the model) takes into account the thermal effects associated with the weak links between granules, the authors do not believe that these effects can explain the observed response. The response amplitude estimated from the kinetic inductivity variation mechanism is also too low (0.04 μ W obtained from theory against an experimental value 100 μ W). However, the experimentally observed response time of about 1 ns is of the same order as the value estimated by using the photofluxon model. For an unambiguous conclusion concerning the applicability of the photofluxon model, we must carry out experiments with a subnanosecond resolution and measure the dependence of the response time on the film thickness, which must be linear.⁹

Salient features and conditions for realization of the mechanism

- (1) The dependence of the resistance associated with the dissociation of the V–AV pairs on temperature and bias current I is obtained by using formulas (16) and (17).
- (2) Formula (15) describes the IVC at different temperatures and for different bias currents.
- (3) The limiting sensitivity of this mechanism is equal to $\Phi_0 / h\nu$.
- (4) The response time for $v_F = 10^7$ cm/s and a film width $w = 10$ μ m is ~ 100 ps.
- (5) The sensitivity can be increased right up to the quantum limit by decreasing the working temperature to below T_{KT} and selecting a film made of uniformly linked small size granules.

2.4. Inverse AC Josephson effect

The emergence of a dc voltage across JJ formed by a low-temperature superconductor under the action of microwave radiation was observed for the first time by Langerberg *et al.*⁵² This phenomenon known as the inverse ac Josephson effect served as an impetus in the study of possible applications of JJ as EMR detectors. The discovery of HTSC stimulated a number of publications^{53–56} in which the observed nonbolometric response of HTSC was interpreted as a modulation of weak-link parameters (critical current, order parameter phase, etc.) by an induced rf current.

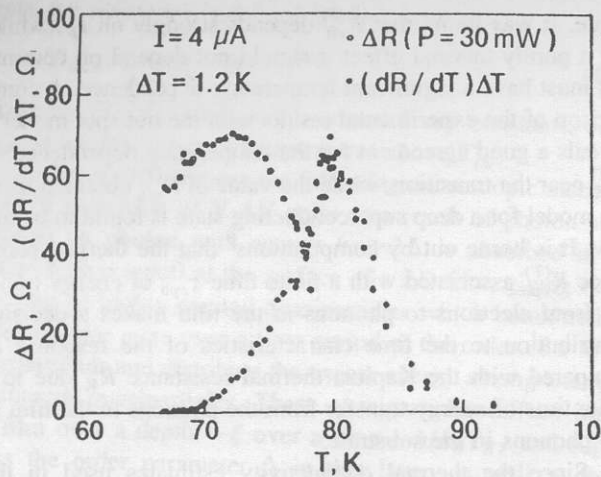


FIG. 5. Temperature dependences of the response ΔR and derivative dR/dT multiplied by the constant $\Delta T=1.2$ K for a YBaCuO film (from Chang *et al.*⁵⁴).

Durny *et al.*⁵³ studied YBaCuO ceramic samples in the form of rectangular bars placed in the cavity of EPR spectrometer. The voltage induced in the sample by MW radiation (9.42 GHz) was measured as a function of temperature T , constant field H , and radiation power P_ω . It was found that the magnetic field suppresses the response for any field polarity. The amplitude ΔV of the response increased with decreasing T and increasing P_ω . The $\Delta V(P_\omega)$ dependence was linear in the P_ω range from 1 to 100 mW at low (~ 31 K) and high (~ 81 K) temperatures. In the intermediate temperature range (50–70 K), weak saturation of the $\Delta V(P_\omega)$ dependence was observed for $P_\omega \sim 20$ –30 mW. Durny *et al.*⁵³ associate the response mechanism with the motion of Josephson vortices formed in weak links under the action of the Lorentz force exerted by the transport current.

Chang *et al.*⁵⁴ studied granular YBaCuO films in the form of an “H”-structure. An “H”-shaped film was placed in a rectangular waveguide so that the electric field \mathbf{E}_ω was parallel to the “bridge,” while the magnetic field \mathbf{H}_ω was perpendicular to the plane of the H-structure. Such an experimental geometry makes it possible to create an optimal coupling with \mathbf{H}_ω and prevents the interaction with the electric component, which permits to avoid ordinary rectification effects which are not associated with the physics of HTSC. A quasi-homogeneous chain of JJ is formed in the bridge of the H-structure, for which the dependence of ΔV on H (or H_ω) is strictly periodic in contrast to a randomly oriented 3D chain, since weak links respond to radiation synchronously. Chang *et al.*⁵⁴ discovered that the temperature dependence of the response $\Delta R=R(P_\omega)-R(0)$ exhibits two peaks (Fig. 5). The high-temperature peak is correctly described by the dependence

$$\Delta R=(dR/dT)\Delta T, \quad (18)$$

typical of the bolometric mechanism. The low-temperature peak of the response is in the tail of the resistive transition, where $dR/dT \rightarrow 0$ and is obviously not of thermal origin. The dependence on microwave power ($P_\omega^{\text{max}} \sim 30$ mW) is linear in the region of the high-temperature peak, which con-

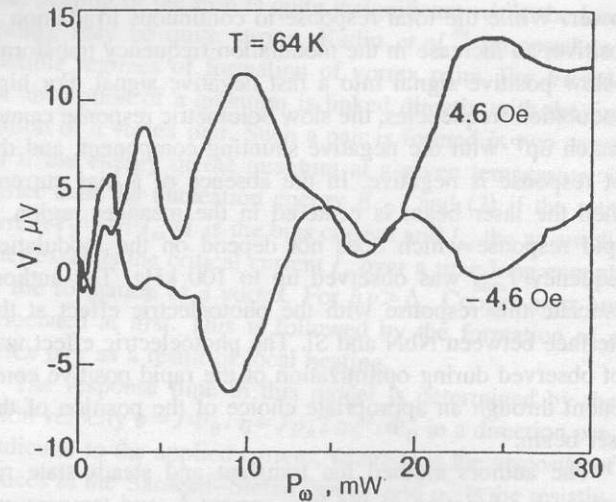


FIG. 6. Dependence of the voltage V induced by microwave radiation on the microwave power of a YBaCuO film in the absence of a constant bias for two different directions of the constant magnetic field at $T=64$ K (from Chang *et al.*⁵⁴).

firms the bolometric nature of the response, while $\Delta R \propto \log(P_\omega)$ in the temperature range in which a nonbolometric response is observed. According to Chang *et al.*⁵⁴ the time variation of the order parameter phase φ induced in a long JJ by MW radiation (even in zero magnetic field) leads to the formation of vortices which can move under the action of a direct transport current. The response amplitude ΔV in this case is proportional to the number of JJ that respond synchronously to radiation for a given I_b . It was found that the nonbolometric peak of the response increases and is displaced towards low temperatures upon an increase in the bias current as well as in the MW power. The response appears under the condition $I_b > I_c$. Chang *et al.*⁵⁴ state that the mechanism of induced motion of vortices proposed by them causes a response similar to that observed during dissociation of V–AV pairs in the course of a Kosterlitz–Thouless transition.⁴⁵ However, the IVC is linear ($V \approx I$) for this mechanism in the vicinity of T_c , while $V \approx I^3$ in the case of dissociation of vortex pairs. In addition, the oscillating dependence of ΔV on P_ω for $H = \text{const}$ (Fig. 6) and on H for $P_\omega = \text{const}$ unambiguously suggest the Josephson mechanism of the response, in which the vortices generated by a weak magnetic field move under the action of the current induced by MW radiation, leading to voltage oscillations.

Gallop *et al.*⁵⁵ observed the dependence of the differential resistance dV/dI of YBaCuO and BiSrCaCuO films on a MgO substrate on the bias voltage V_b under the effect of MW radiation (~ 10 mW) of frequency 8–20 GHz. The difference in the differential resistance in the presence of radiation and without it is of a periodic oscillating form with peaks at $V_b = n\Phi_0\nu$, where n is an integer and ν the radiation frequency. We assume that the fluxon lattice observed in YBaCuO at low temperatures moves under the action of the rf current, which induces the voltage $V = d\Phi/dT = m\nu(I_b\Phi_0)$ according to Faraday’s law (m is the number of fluxons per unit area and $\nu(I_b)$ the velocity of fluxons, which strongly depends on the bias current I_b). The motion of flow

in this case is synchronized with the applied MW voltage within a limited range of V_b so that the velocity of fluxon motion through a superconducting microstrip is $dN/dt = n\nu$. In this case, the voltage drop across the film in this synchronized state is $V = \Phi_0(dN/dt) = n\Phi_0\nu$. This condition is similar to the condition for the formation of a Shapiro step in a solitary JJ.

Boone *et al.*⁵⁶ also studied the response of YBaCuO films in the form of $2000 \times 600 \mu\text{m}$ strips of thickness 1.3–2 μm to pulsed MW radiation of frequency 9 GHz. The response observed in the region of resistive “tail” increases with I_b and with MW power ($P_{\omega}^{\text{max}} \sim 100 \text{ mW}$). It was found that the response amplitude is independent of the modulation frequency, which is typical of a nonbolometric response. The noise voltage measured with the help of a synchronous detector (in the absence of radiation), as well as the response itself, had a peak in the region of the resistive tail. The noise measurements permitted the estimation of the noise equivalent power (NEP) $P_{\text{eq}} \sim 6 \cdot 10^{-10} \text{ W}/\sqrt{\text{Hz}}$, the responsivity being 136 V/W. Among possible mechanisms of response, the radiation-induced flux flow within intergranular weak links is considered. The mechanisms of dissociation of V–AV pairs,⁴⁵ photoinduced flux creep,¹⁷ and synchronization of the fluxon lattice with the MW field⁵⁵ are not ruled out either.

Huggard *et al.*⁵⁷ studied the response of BiSrCaCuO thin-film bridges to the pulsed ($\tau = 65 \text{ ns}$) IR radiation ($\Lambda = 447 \mu\text{m}$) with the pulse repetition frequency of 165 Hz. The observed broadening of the decreasing component to the output pulse as compared to the input pulse can be explained by the nonlinearity of the response. As the current I_b increases, the peak of the response corresponding to the end of the resistive tail was shifted towards low temperatures right up to complete vanishing of the response for $I_b > 100 \mu\text{A}$. The amplitude of the response was proportional to $\sqrt{P_{\omega}}$ in the case of high radiation powers and was linear in P_{ω} for low powers. The two methods of estimating NEP and responsivity mentioned above lead to the following results: $P_{\text{eq}} = 5 \cdot 10^{-9} \text{ W}/\text{Hz}^{1/2}$, $R_v = 0.6 \text{ V}/\text{W}$ ($1 \text{ mW} < P_{\omega} < 50 \text{ mW}$) and $P_{\text{eq}} = 3 \cdot 10^{-12} \text{ W}/\text{Hz}^{1/2}$, $R_v = 1.2 \cdot 10^{-2} \text{ V}/\text{W}$ ($0 < P_{\omega} < 1 \text{ mW}$). All the estimates were obtained in a detection band of 50 MHz. Huggard *et al.*⁵⁷ ruled out the bolometric origin of the response since, according to Barone and Paterno,⁵⁹ the critical current is independent of temperature at $T < T_c/3$, while the response in Ref. 57 was observed at $T = 17 \text{ K} \ll T_c/3$ ($T_c \sim 85 \text{ K}$).

Computer simulation proved⁵⁸ that for frequencies $h\nu \ll 2\Delta$ and $I_{\omega}/I_0 < 1$, the maximum nondissipative current $I_c = I_0(1 - \gamma I_{\omega})$, where γ is a constant, I_{ω} the amplitude of the current induced by radiation, and I_0 the characteristic spread in the critical currents of JJ forming a bridge. At a working point with the differential resistance $\delta V/\delta I = R$, the voltage across the junction satisfies the equation

$$V = \gamma I_0 R I_{\omega}, \quad (19)$$

or $V \sim \sqrt{P_{\omega}}$. For $I_{\omega} \ll I_0$, a linear dependence on P_{ω} is expected.⁵⁹ Thus, Huggard *et al.*⁵⁷ proved that the response of a bridge to IR radiation is correctly described by the

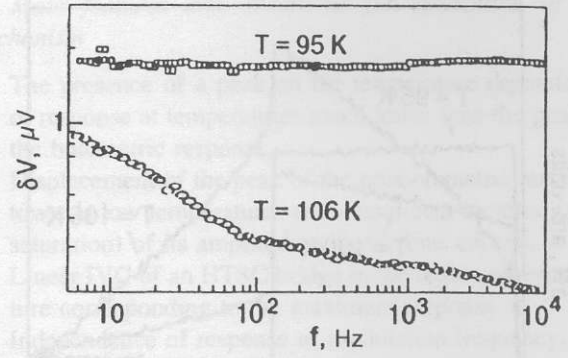


FIG. 7. Photoresponse of a BiSrCaCuO thin film as a function of the modulation frequency for the bolometric ($T = 106 \text{ K}$) and nonbolometric ($T = 95 \text{ K}$) components, $I = 1 \text{ mA}$ and $P = 2.5 \text{ mW}/\text{cm}^2$ (from Ngo Phong and T. Shih⁶²).

model of a solitary JJ in which I_c is replaced by a certain effective value I_0 . This confirms the hypothesis on synchronous response of weak links to EMR.⁶⁰

Schneider *et al.*⁶¹ studied the frequency dependence of the response of BiSrCaCuO microbridges in the frequency range (10–1000) cm^{-1} . For frequencies varying from 10 to 100 cm^{-1} , only a nonbolometric response with a time constant $\tau \sim 4 \text{ ns}$ was detected with the dependence $\Delta V \sim P_{\omega}^{1/2}$ in the range from 3 to 30 mW. At a frequency 939 cm^{-1} , a bolometric response is also observed in addition to the nonthermal component near T_c . For $P_{\omega} < 1 \text{ mW}$, both components are linear functions of power. In this case, the response amplitude $\Delta V \sim \sqrt{P_{\omega}}$ for $\omega < 100 \text{ cm}^{-1}$, while this quantity is proportional to P_{ω} for $\omega = 939 \text{ cm}^{-1}$. The frequency dependence of the response in the frequency range from 10 to 1000 cm^{-1} is correctly described by a power law with the exponent 2.3. The obtained results confirm the Josephson nature of the nonbolometric response and rule out nonequilibrium mechanisms associated with electron heating and hot spots exhibiting a linear power dependence and a weak frequency dependence.

Ngo Phong and T. Shih⁶² measured the response of strip structures of BiSrCaCuO granular films to 5-mm radiation. The response had high-temperature bolometric and low-temperature nonthermal components. The heating near T_c was estimated at $\sim 0.3 \text{ mK}$. With increasing bias current, the dynamics typical of both components was observed: the high-temperature component of the response increased linearly and remained at the same temperature, while the low-temperature component increased nonlinearly, attaining saturation for large values of I_b , and was shifted towards lower temperatures. The high-temperature component as a function of modulation frequency decreased abruptly in the range $0 < f_{\text{mod}} < 100 \text{ Hz}$ and then diminished more smoothly up to 10 kHz. At the same time, the low-temperature component was virtually independent of f_{mod} (Fig. 7). The transformation of the MW pulse ($\tau \sim 50 \text{ ms}$) after the interaction with the sample was also studied at three temperatures (Fig. 8). In the region of low-temperature component, the shape of the output pulse was exactly the same as that of the input pulse, demonstrating a short response time (the leading front $< 250 \text{ ns}$). The high-temperature component was character-

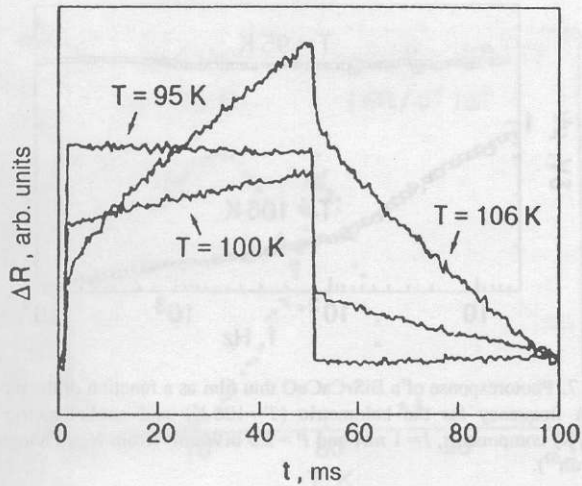


FIG. 8. Transient response ΔR of a thin YBaCuO film induced by MW ($\Lambda=5$ mm) pulsed radiation at various temperatures near T_c , $I=1$ mA, $f_{\text{mod}}=10$ Hz, and $P=2.5$ mW/cm² (from Ngo Phong and T. Shih⁶²).

ized by a "smeared" asymmetric output pulse (the rise and fall times ~ 1 ms and ~ 20 ms respectively). For the intermediate temperature, the steepness of the leading front of the output pulse varied with time, indicating the presence of a thermal as well as a nonthermal component in the response. The amplitude of the nonthermal component decreased with the extent of granular structure in the sample, and the nonbolometric response was not observed at all for samples with $J_c \sim 10^5$ A/cm² at 77 K. The estimates of responsivity and detectability D^* under nonbolometric conditions give the values of $R_v=10$ V/W and $D^*=1.1 \cdot 10^8$ cm·Hz^{1/2}/W. For both components, the power dependence was linear. A dependence of the form $\Delta V \sim P^{1/2}$ typical of JJ for large values of power⁵⁹ was not observed since large power levels were inaccessible. Finally, an analysis of the temperature dependence of the optical ($\Lambda \sim 1.06$ μm and $\Lambda \sim 1.56$ μm) and MW ($\Lambda \sim 5$ mm) responses in the same sample showed that only the bolometric component is left for $h\nu > 2\Delta$. It was emphasized that the Josephson detection mode is typical only for $h\nu < 2\Delta$.

Schneider *et al.*³ studied recently the response of microstrips made of BiSrCaCuO films on MgO substrates to pulsed (~ 80 μs) IR radiation ($\Lambda \approx 0.5$ mm) in a constant magnetic field up to 8 T. The magnetic field dependence of the response is determined by the dependence of critical current on B for a solitary rectangular JJ of thickness $d \ll \lambda_L$ and length l in a transverse magnetic field:

$$I_c(B) = I_c(0) \left| \frac{\sin[\pi(\Phi/\Phi_0)]}{\pi(\Phi/\Phi_0)} \right|. \quad (20)$$

The interference pattern is blurred in view of the spread in the parameters of weak links. Schneider *et al.*³ proved that, according to (20), the magnetic field can either suppress ($I_b > I_c$) or enhance ($I_b < I_c$) the response depending on the relation between I_b and I_c for I_b varying from 2 to 100 μA in the magnetic field range 1 mT $< B < 50$ mT. Since $I_c(B)$ depends on the length of the junction, Schneider *et al.* could estimate the characteristic size of junctions ($l_j \approx 0.5$ μm).

For $B < 50$ mT, the $\Delta V(B)$ dependence has a plateau which is attributed by the authors to the presence of weak links of the nanometric scale with considerably higher values of I_c , which are "immersed" in grain boundaries. The characteristic size of such "strong" weak links, which was estimated from the period of the diffraction pattern, is $l_a \leq 1$ nm. The dependence of the response on H also exhibits a hysteresis (memory effects), and the response remains suppressed for $I_c > 20$ μA even after the removal of the field. This can be due to flux trapping in the network of granules and to the presence of weak links with high values of I_c , which form a barrier preventing the escape of vortices. However, Schneider *et al.*³ rule out the trapping in granules themselves since it would decrease the intergranular field and lead to stimulation rather than suppression of the response.

Irie and Oya⁶³ studied in 1995 the response of BSCCO single crystals having a size of 1×1 to 3×5 mm and thickness 0.1–0.2 mm to MW radiation (of frequency 8–10 GHz). The measurements of the response by the four-probe technique along the c -axis revealed that the IVC of an exposed sample contains multiple resistive branches which are attributed by the authors to interplanar chains of series-connected JJ of the SIS type in the single crystal. For $I_b > I_c^{\text{min}}$, a voltage is induced across the weakest junction, and a further increase in I_b leads to the formation of N jumps on IVC, corresponding to transition to the resistive state in N Josephson junctions. For low radiation power levels, the steps on IVC satisfy the relation $V_n = mn\nu/2e$, where m is the number of synchronized junctions, n is an integer (number of steps), and the shape of the IVC is similar to that for a solitary JJ. In the case of high-intensity radiation, when the signal frequency coincides with one of bulk modes of the resonator, the IVC changes significantly. It acquires steps corresponding to synchronization of fluxons with MW radiation. Finally, for large values of power, when the MW frequency does not coincide with resonator modes, vortices are not synchronized with external radiation. In this case, the flux flow mode can dominate over Josephson properties of the junction, which is also confirmed by the power dependence of the height of voltage steps, having the form $V_n \sim P_\omega^{1/2}$. In this case, neither the voltage V_p corresponding to the formation of steps, nor the amplitude I_p of a step depend on frequency in the range 8–10 GHz. In this case, the steps are considerably blurred (broadened) since the motion of fluxons is not associated with resonant modes, and irradiation plays the role of a trigger that controls the arrival of vortices in the junction.

Ling *et al.*⁶⁴ used the four-probe technique to study the response of YBaCuO single crystals to MW radiation (8–12 GHz) with or without direct measuring current along the c -axis. The sample was mounted at the end of the waveguide so that the MW fields H_ω and E_ω were parallel to the (ab) plane and the c -axis, respectively. The sliding short located at the end of the waveguide made it possible to control the position of the peaks of the electric and magnetic fields relative to the sample.

The dependence of response on the bias current in the normal state ($T=94$ K) for various radiation powers (from 1 to 7 mW) was linear with a negative slope due to the fact that

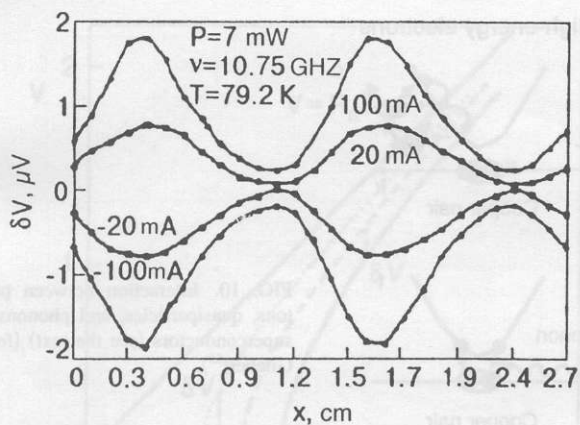


FIG. 9. Constant voltage δV induced by microwave radiation as a function of the sample coordinate for a strong current (from Ling *et al.*⁶⁴).

the resistance along the *c*-axis in the normal state varies in proportion to $1/T$. In the superconducting state, the dependence of response on I_b has the shape of a curve with a peak displaced towards smaller currents upon an increase in the power P_ω . The response has positive polarity and an amplitude two orders of magnitude larger than in the normal state. At the same time, the current corresponding to the maximum response is equal to the critical current. The dependence of the response along the *c*-axis on the position x of the sample exhibits bipolar oscillating behavior with a period equal to $1/2$ wavelength in the waveguide. The frequency dependence of the response in the range 8–12 GHz is also oscillating. This rules out rectification and differential heating associated with sample inhomogeneity as possible reasons of the response. On the other hand, such a behavior is in accord with ordinary time-dependent Josephson effect in which induced voltage varies as a Bessel's function. For $I_b=0$, no correlation between the ΔV peaks and the components E_ω and H_ω of the MW field was observed, while an increase in I_b led to clearly manifested displacement of oscillatory peaks towards maxima of the magnetic field H_ω . The height of the peaks increased with the bias current, and for large values of I_b (>20 mA) the polarity of the peaks was strictly determined by the polarity of bias current (Fig. 9). Ling *et al.*⁶⁴ attribute the observed response to the presence of intrinsic Josephson junctions in YBaCuO in the direction of the *c*-axis, in which the NW radiation induces pairs of Josephson vortices and antivortices. If $I_b \neq 0$, the formed pair of vortices is carried by current in various directions, leading to the emergence in the sample of a voltage with polarity coinciding with the polarity of I_b . For $I_b \neq 0$, the peaks of the response must coincide with the peaks of H_ω , and the polarity must be the same as that of I_b .

For $I_b=0$, vortices move under the action of MW electric field E_ω with a phase shift θ relative to H_ω in view of different phase relations for H_ω and E_ω in the Josephson junction. The resultant pattern of $\Delta V(x)$ depends on θ and has peaks separated by $\Lambda/2$. The polarity changes with the position x of the sample and can be purely positive or negative for $\theta = \pm \pi/2$.

Main features and conditions for realization of the mechanism

- (1) The presence of a peak on the temperature dependence of response at temperatures much lower than the peak of the bolometric response.
- (2) Displacement of the peak of the nonbolometric response towards low temperatures and a nonlinear increase (with saturation) of its amplitude with the bias current.
- (3) Linear IVC of an HTSC bridge in the region of temperature corresponding to the maximum response.
- (4) Independence of response of modulation frequency.
- (5) Increase in the response amplitude with the extent of granular structure in the sample.
- (6) Decrease in the response amplitude with the radiation frequency approximately in proportion to $\omega^{2.3}$.
- (7) Linear and root dependence on radiation power for large and small power levels respectively.
- (8) Stimulation of the response by a weak magnetic field for $I_b < I_c$ and its suppression for $I_b > I_c$.

2.5. Nonequilibrium breaking of cooper pairs

The properties of a superconductor below T_c are very sensitive to external excitations such as electrons, phonons, and photons.⁶⁵ In the case of MW frequencies for which $h\nu < 2\Delta$. Cooper pairs cannot be broken, and the absorption of a photon is reduced to the energy redistribution of quasiparticles, which can stimulate superconductivity under certain conditions due to an increase in the gap width.^{66,67} Cooper pairs can break under the interaction of the superconductor with EMR whose energy quantum $h\nu > 2\Delta$ (light and IR radiation). Optical photons have energy of the order of several eV, while the energy corresponding to the gap in typical HTSC is of the order of tens of meV (e.g., the gap $2\Delta \approx 30$ meV for YBaCuO).

The interaction between optical radiation and a superconductor is presented in Fig. 10.⁶⁵ Photons incident on a superconductor break Cooper pairs and generate quasiparticles with energies $E \gg 2\Delta$ (see Fig. 10a). Electrons possessing such high energies relax very rapidly (through electron–electron and electron–phonon collisions) to states with energies in the range of the gap energy (see Figs. 10b and c). An absorption of a photon generated a large number of quasiparticles and phonons in the range of energy gap during a very short period of time (see Fig. 10d). The recombination of excited quasiparticles is accompanied by the creation of Cooper pairs and emission of phonons (see Fig. 10e). Pair breaking by phonons with energies $> 2\Delta$ occurs during the characteristic time τ_B (see Fig. 10f). Over the time τ_{es} , phonons escape from the film to the substrate (see Fig. 10g). Other processes with their own characteristic times also exist, including the scattering of excited quasiparticles accompanied with absorption (see Fig. 10h) or emission (see Fig. 10i) of a phonon. The time of energy relaxation of electrons through the electron–phonon interaction is an important parameter characterizing the intensity of this interaction.

Nonequilibrium effects in HTSC materials are mainly observed in structures with Josephson properties (bridges and junctions in edge steps as well as bicrystalline sub-

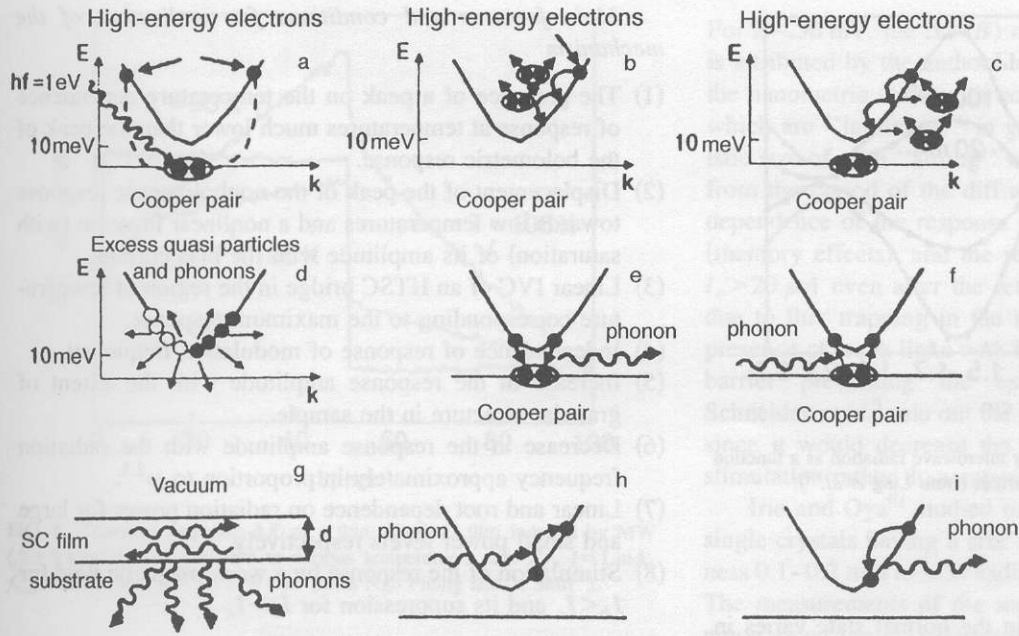


FIG. 10. Interaction between photons, quasiparticles, and phonons in superconductors (see the text) (from Gilibert⁶⁵).

strates). In spite of considerable technological difficulties associated with a small length ξ in HTSC materials, Josephson structures with quite reproducible properties, such as junctions at edge steps, can be obtained even now by using various artificial approaches. Sometimes, the region of a weak link in such structures is coated by a photoconducting layer (usually CdS) in order to improve the sensitivity of the detector and to prevent the degradation of the sample.⁶⁵

Enomoto *et al.*⁶⁸ studied the response of thin ($\sim 0.2 \mu\text{m}$) BaPbBiO films ($T_c = 13 \text{ K}$) to IR radiation. It is well known that the critical current of JJ is determined by the Ambegaokar–Baratov relation $I_c = \pi\Delta/(2eR)\tanh(\Delta/2k_B T)$, and at $T \ll T_c$ we have $I_c \approx \pi\Delta/2eR$. Irradiation of the superconductor leads to a change in the critical current $\delta I_c \approx (\pi\delta\Delta)/2eR$, where the change in the energy gap is connected with the number of excess quasiparticles through the relation $\delta\Delta = \delta n/N(0)$. Thus, knowing the change in critical current, we can find the change in the energy gap and the number of excess quasiparticles. Figure 11 shows schematically the IVC for a tunnel JJ exposed to radiation and without it. In the RSJ model, the IVC of a weak bond is described by the formula⁶⁵

$$V = R(I^2 - I_c^2)^{1/2}. \quad (21)$$

This leads to the following expression for the photoresponse of the weak coupling:

$$\Delta V = -\frac{RI_c \delta I_c}{(I^2 - I_c^2)^{1/2}} = \frac{-\pi I_c \delta\Delta}{2e(I^2 - I_c^2)^{1/2}} \quad \text{for } I > I_c \quad (22)$$

and

$$(\Delta V)_{I=I_c} = R(2I_c \delta I_c)^{1/2} = \frac{\pi}{e} (\delta\Delta/2)^{1/2} \quad \text{for } I \leq I_c. \quad (23)$$

The variation of the IVC for a weak link under radiation is shown in Fig. 12a, and the response as a function of bias current together with the dependence calculated by formulas (21)–(23) is presented in Fig. 12b.

Later, Tanabe *et al.*,⁶⁹ who studied the response of bridges made of thin YBaCuO and LaSrCuO films to pulsed optical radiation ($\lambda \sim 1.3 \mu\text{m}$), detected a fast component in the response. The dependence of the response voltage ΔV on I_b had a peak which became narrower and higher upon cooling. With increasing I_b , the peak on the temperature dependence of the response increased and shifted to lower temperatures. The responsivity for the nonbolometric response associated with pair breaking is described by the formula

$$R_{NE} = \frac{\delta V}{\delta I_c} \bigg|_{I_c} \frac{\delta I_c}{\delta \Delta} \bigg|_T \frac{\delta \Delta}{n_{qp} T} \frac{\delta n_{qp}}{P}, \quad (24)$$

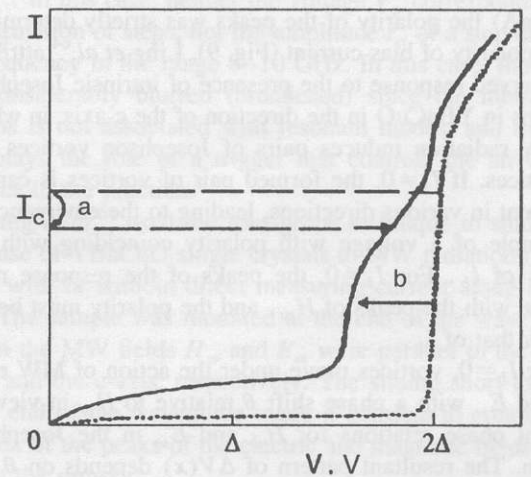


FIG. 11. Typical IVC of a Josephson tunnel junction. Solid and dashed curves represent IVC with irradiation (a) and without it (b) (from Gilibert⁶⁵).

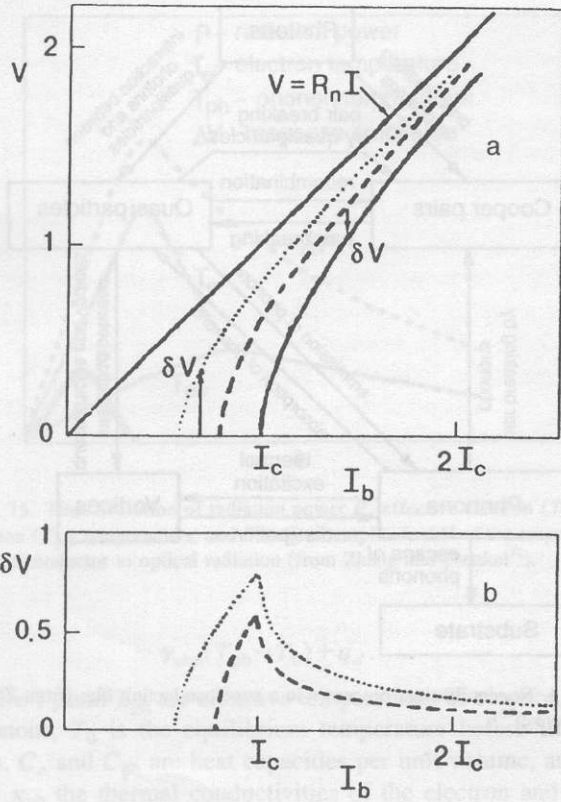


FIG. 12. Effect of radiation on a weak link: the solid curve corresponds to IVC in the absence of radiation, while the dashed and dotted curves correspond to irradiation (a); dependence of the voltage shift δV on the bias current I_b for two characteristics $V(I)$ (dotted and dashed curves) (b) (from Gilibert⁶⁵).

where n_{qp} and P are the number density of quasiparticles and radiation power respectively. The first cofactor in (24) defines the dependence on the bias current I_b , while the temperature dependence is presented by the second and fourth cofactors. The third cofactor can be expressed in terms of the density of states N as $\delta\Delta/\delta n_{qp} = 1/2N(0)$. The second cofactor follows the temperature dependence of the critical current, which determines the general temperature dependence of the response. Consequently, the overall temperature dependence is mainly determined by the dependence $I_c(T)$, which was just observed by Tanabe *et al.*⁶⁹ According to Tanabe, the value of responsivity is mainly determined by the cofactor $N(0)\Delta/2$. The experiments with YBaCuO and LaSrCuO films give the value of responsivity ~ 20 – 30 V/W at low temperatures (~ 5 K), while the value of responsivity for similar BaPbBiO films is two orders of magnitude higher. The authors explain this by a considerable difference in the population densities for these two classes of superconductors and assume that the breaking of Cooper pairs by radiation is the basic mechanism of the response.

Johnson⁷⁰ studied thin YBaCuO films (20–200 nm) with high values of J_c ($> 10^5$ A/cm²) in quasi-two-dimensional geometry. The response to optical radiation ($\Lambda \approx 665$ nm) with a pulse duration 0.3 ps and pulse repetition frequency 2 kHz was recorded with the help of ultrahigh-speed oscilloscope (10 ps $< t < 10$ ns). It was found that the response contains two component: in the vicinity of $T_c \pm \Delta T/2$ (where

$\Delta T = 3$ K is the superconducting transition width), a bolometric signal with a time constant ~ 3 ns was observed, which increases linearly with the bias current I_b as well as with the radiation power. The second component observed at $T < T_c - \Delta T/2$ has a fall time ~ 100 ps and is characterized by a steeper than linear dependence on P and I_b with saturation for large values of the argument. In spite of the fact that the position of the peak on the low-temperature component was exactly the same as for the peak of dR/dT , the response was almost two orders of magnitude stronger than the bolometric signal and was virtually independent of temperature at low temperature for which $dR/dT \rightarrow 0$. Besides, the response decreased with time much more rapidly (~ 100 ps) than the bolometric component (~ 3 ns) at $T > T_c - \Delta T/2$. Johnson drew the conclusion that the observed response is associated with photoinduced breaking of Cooper pairs.

A nonbolometric response was also observed by some authors in HTSC epitaxial films.⁷¹ The optical response in the femtosecond range studied with the help of the ‘‘pump-probe’’ method (see Sec. 1) demonstrated the avalanche multiplication of quasiparticles following the absorption of a photon.¹⁴ This process is associated with inelastic electron–electron scattering on the time scale $\tau_{ee} \leq 1$ ps. Quasiparticles also interact with phonons through inelastic electron–phonon scattering. This loss mechanism is associated with the energy gap suppression as well as with the motion of vortices. A decrease in the number density of Cooper pairs also leads to a change in the kinetic inductance, which also affects temporal characteristics of the response.⁷²

Han *et al.*⁷³ studied the dynamics of a femtosecond response in YBaCuO films of thickness 100–500 nm on a SrTiO₃ substrate. They used a laser with a pulse duration ~ 60 fs, $\Lambda = 625$ nm, and the pulse repetition frequency 80 MHz. The typical shape of transient response signal at $T > T_c$ and $T < T_c$ is shown in Figs. 13a and 13b respectively. In the normal state, the response ΔR is positive. It emerges abruptly during the time ~ 1 ps and decreases slowly over ~ 3 ns. A comparison of the response with dR/dT revealed its bolometric origin. At the same time, the transient response is negative at $T < T_c$ with a rise time ~ 300 fs and with a rapid fall to zero over 7–8 ps. After this the response becomes positive due to the thermal effect associated with diffusion of phonons (in analogy with the response at $T > T_c$). It was found that the temperature dependence of the peak height of the response is successfully approximated by the two-fluid model and has the form $[1 - (T/T_c)^4]$. Han *et al.*⁷³ proposed that the optical response mechanism includes the two main processes: (1) avalanche multiplication of quasiparticles following the absorption of a photon, and (2) nonlinear recombination of photogenerated quasiparticles. Han *et al.*⁷³ also noted that the quasiparticle response is observed only when the system is not saturated. Indeed, the maximum number density of photoinduced quasiparticles estimated from the data on radiation intensity proved to be an order of magnitude smaller than the characteristic density of states in HTSC materials ($N_s \sim 10^{21}$ cm⁻³). The authors of Ref. 73 also noted that the recombination rate ν increases slightly in the interval from 0 to $T_c/2$ and then decreases rapidly. This is explained by the fact that the recombination

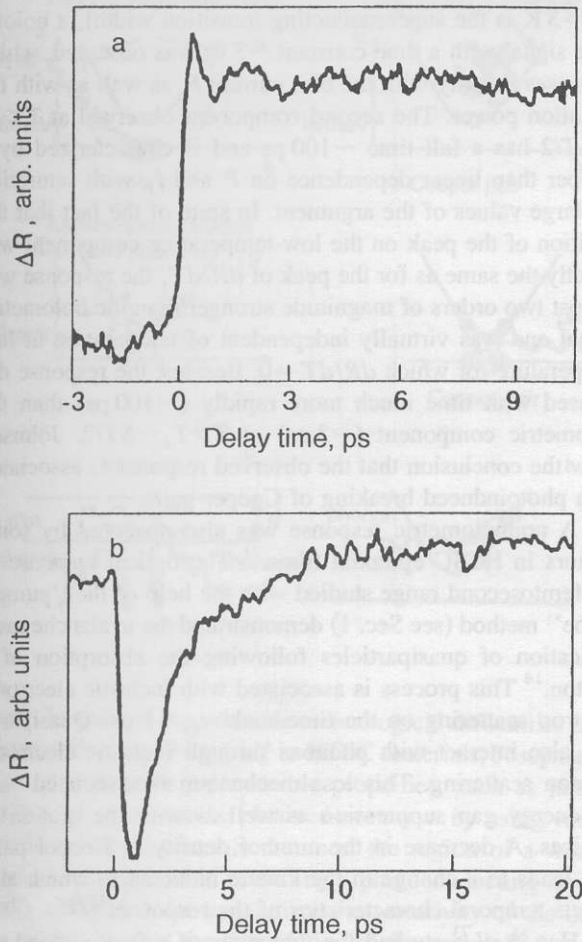


FIG. 13. Transient response ΔR of an epitaxial YBaCuO film at $T = 300$ K (a) and 20 K (b) ($T_c = 93$ K) (from Han *et al.*⁷³).

of quasiparticles is accompanied by the generation of optical phonons that interact resonantly with the gap. The latter circumstance leads to a decrease in the gap width and to softening of this resonant interaction. The decrease in the gap width in turn is manifested directly in a decrease in the recombination rate.

Analyzing the femtosecond dynamics of the optical response, Sobolewski *et al.*¹⁵ proved that the response of YBaCuO epitaxial films of thickness 80–250 nm has a characteristic time ~ 30 ps and can be explained in the thermomodulation model according to which hot holes are generated by radiation. A redistribution of these holes leads to a displacement (rise) of the Fermi level E_F in copper–oxygen planes, resulting in the emergence of a response. A decrease in the oxygen concentration in the film lowers E_F . If the energy of a probing radiation quantum is lower than the Fermi level (in the initial state), the value of E_F increases upon irradiation. The polarity of the response signal must change at the instant of crossing the energy level corresponding to the energy of the beam, which was actually observed by Sobolewski *et al.*¹⁵ and by Han *et al.*⁷³ (see Figs. 13a and 13b). If, however, the value of E_F is initially higher than the energy of the beam, the polarity of the response remains unchanged (positive; see Fig. 13a). Sobolewski *et al.*¹⁵ emphasize that the application of the thermomodulation model

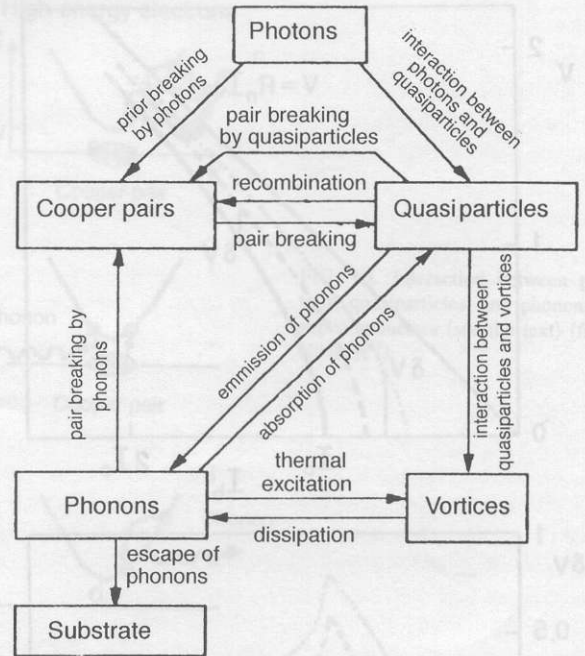


FIG. 14. Nonequilibrium processes in a superconducting film (from Zhang and Frenkel⁷²).

is justified only for $\text{YBa}_2\text{Cu}_3\text{O}_{6+x}$ with the oxygen concentration $x > 0.4$.

It should be stressed that vortices in type II superconductors, can also be involved in the optical response dynamics in addition to quasiparticles and phonons. The block diagram illustrating all possible types of interactions between these three subsystems is shown in Fig. 14. The processes occurring in the superconductor in this case can be explained as follows⁷²: (1) photons interact with Cooper pairs and quasiparticles, generating electrons having a higher energy (the photon–electron interaction occurs during a time ~ 1 fs); (2) high-energy quasiparticles continuously break new Cooper pairs and generate extra quasiparticles during the time τ_{ee} ; (3) quasiparticles interact with phonons through the absorption and emission of phonons (τ_{eph}); (4) high-energy phonons break Cooper pairs (τ_B); (5) quasiparticles recombine into Cooper pairs and generate phonons (τ_B); (6) quasiparticles and phonons activate the motion of vortices, leading to dissipation (the corresponding time scales of these processes are denoted by τ_{ev} , τ_{phv} , and τ_d); (7) phonons escape from the film to the substrate over the time τ_{es} of the order of nanoseconds.

According to Anisimov *et al.* and Qui and Tien,⁷⁴ the electron and phonon subsystems can be assumed to be in equilibrium with each other. The effective temperatures of the electron and phonon gases are given by⁷⁵

$$C_e \frac{dT_e}{dt} = \kappa_e \nabla^2 T_e - \gamma_{eph}(T_e - T_{ph}) - \gamma_{ev}(T_e - T_0) + q_{ab} \quad (25)$$

and

$$C_{ph} \frac{dT_{ph}}{dt} = \kappa_{ph} \nabla^2 T_{ph} + \gamma_{eph}(T_e - T_{ph})$$

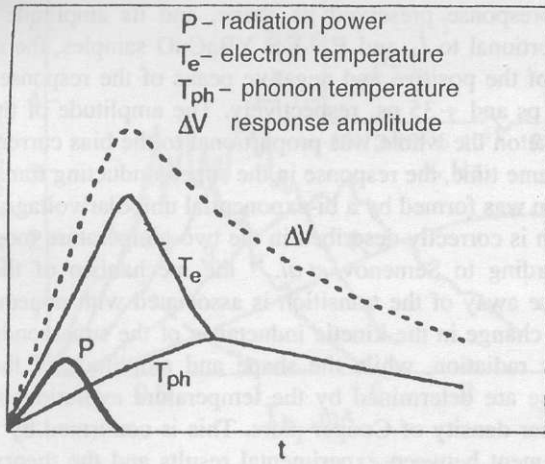


FIG. 15. Time evolution of radiation power P , effective electron (T_e) and phonon (T_{ph}) temperatures, and the signal amplitude ΔV of the response of a superconductor to optical radiation (from Zhang and Frenkel⁷²).

$$-\gamma_{phv}(T_{ph}-T_0)+q_d. \quad (26)$$

where T_e and T_{ph} are effective temperatures of electrons and phonons, T_0 is the equilibrium temperature before irradiation, C_e and C_{ph} are heat capacities per unit volume, and κ_e and κ_{ph} the thermal conductivities of the electron and phonon subsystems respectively, γ_{eph} , γ_{ev} , and γ_{phv} are the electron-phonon, electron-vortex, and phonon-vortex coupling constants respectively, and q_{ab} and q_d are the absorbed and scattered power densities. The solution of this system of equations makes it possible to calculate the enhancement in the electron temperature relative to the phonon temperature as a result of irradiation. When the duration of radiation pulse is $\tau \gg \tau_{eph}$, the electron temperature approaches the phonon temperature. For $\tau \gg \tau_{ee}$ and τ_{eph} , the effective temperatures of electrons and phonons are approximately equal. Figure 15 shows the dynamics of the most important characteristic times as well as the input pulse, when the duration of the latter is shorter than the electron-phonon relaxation time. It can be seen that the value of T_e attains the peak at the end of optical pulse, and the peak of the response corresponds to the peak of T_e . According to Frenkel,⁷⁵ the thermal relaxation time determined by the time τ_{es} during which phonons escape to the substrate can be reduced by eliminating the resistance of the "film-substrate" thermal interface by using narrow superconducting microstrips as detectors. The sensitivity in the bolometric mode can be improved by enhancing pinning in operation with large bias currents. However, the mechanisms of interaction between electrons and vortices, phonons and vortices, as well as vortex dissipation have not been studied completely so far.

Gol'tsman *et al.*⁷ studied the response of YBaCuO films prepared by laser ablation on various substrates to pulsed ($\tau \sim 20$ ps) optical ($\lambda = 0.63$ and $1.54 \mu\text{m}$) radiation with a pulse repetition frequency 0.5 Hz. The time dependence of transient response has the form of a solitary pulse with steep left slope (of the order of several ps) corresponding to the nonequilibrium component and a "smeared" (tens of ps) right slope corresponding to the bolometric component (Fig. 16). The peak of the response amplitude corresponds to the

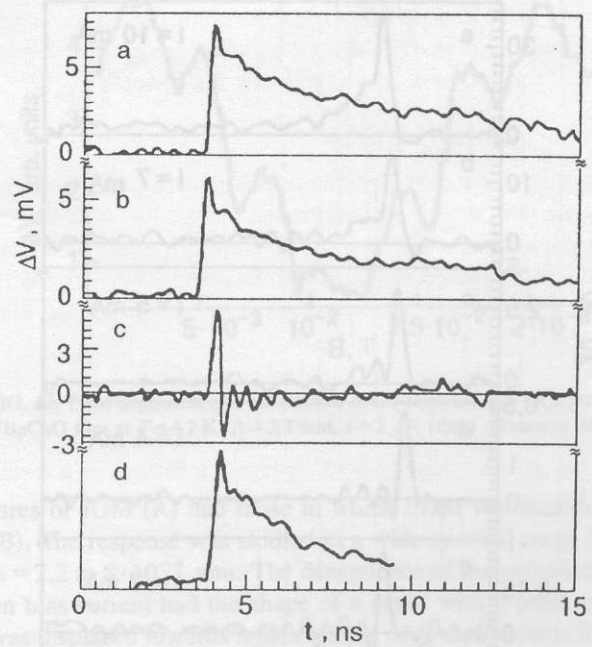


FIG. 16. Transient response of a YBaCuO microbridge at various temperatures (a-c): $T = 100$ K (normal state, $I_b = 7.5$ mA, $E = 40 \mu\text{J}/\text{cm}^2$) (a); $T = 85$ K (near the middle of the junction, $I_b = 1$ mA, $E = 2 \mu\text{J}/\text{cm}^2$) (b); $T = 54$ K (superconducting state, $I_b = 1$ mA, $E = 40 \mu\text{J}/\text{cm}^2$) (c); the integral of the curve in Fig. 16c with respect to time (d) (from Gol'tsman *et al.*⁷).

steepest part of the superconducting transition. The shape of the right slope first followed an exponential law, and then a power law identified with a rapid bolometric effect and thermal diffusion to the substrate. Since the time constant corresponding to the exponential decay is proportional to the film thickness, Gol'tsman *et al.*⁷ explain this process by the escape of nonequilibrium phonons to the substrate. When nonequilibrium phonons return to the film, a transition from the rapid bolometric effect to diffusion flow with power attenuation takes place. As the temperature decreases ($T = 54$ K), the ratio of the amplitudes of fast and slow components increases, and a signal with negative polarity is formed simultaneously. The response integrated with respect to time is exactly similar to the response in the normal and resistive states, but is characterized by a larger ratio of the amplitudes of the fast and slow components (Fig. 17).

A similar behavior is observed in the dependence of the response shape in the superconducting state on the displacement current at constant temperature. At first ($I_b = 2$ mA), the negative component decreases, and then vanishes altogether, while the positive component appears. For large values of I_b (~ 10 mA), the wavy shape of the response resembles that in the resistive and normal states. The authors draw the conclusion that a nonequilibrium picosecond component is observed in all the three states. In the normal state, photoexcited charge carriers possess a lower scattering rate than in the equilibrium state, which leads to a decrease in the mobility of charge carriers and hence to an increase in resistance. In the superconducting state, the nonequilibrium response is associated with a change in kinetic inductance. However, in the resistive state (in the superconducting transition region), the inductive and resistive components coex-

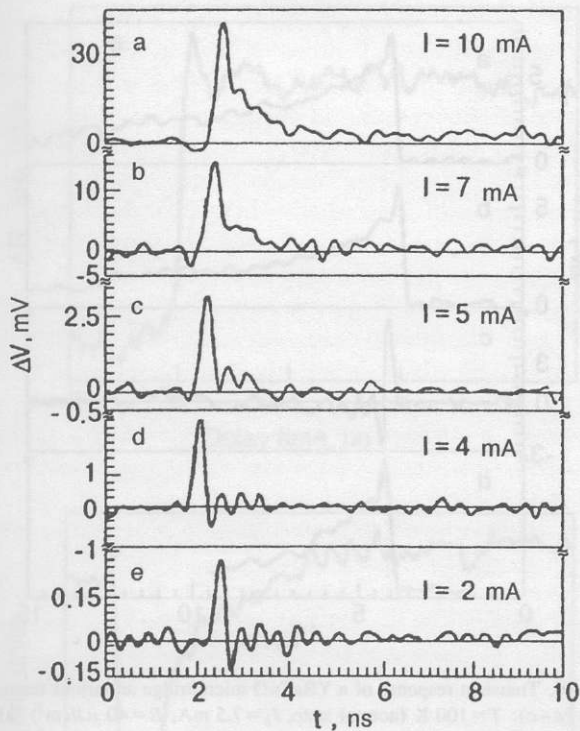


FIG. 17. Transient photoresponse of a YBaCuO microstrip line at $T = 4.2$ K, $E = 2 \mu\text{J}/\text{cm}^2$ and various bias currents I_b , mA: 10 (a), 7 (b), 5 (c), 4 (d), and 2 (e) (from Gol'tsman *et al.*⁷).

ist. It was also found that the ratio of the amplitudes of the nonequilibrium and rapid bolometric components virtually does not change during a transition from the normal to the superconducting state. This means that none of superconducting peculiarities affects the shape of a transient pulse, and only the magnitude of the nonequilibrium component commensurate with the bolometric component is affected. This feature is typical of the effect of suppression of the gap by excess quasiparticles generated by irradiation, which results in an increase in resistance in the normal and resistive states or an increase in the kinetic inductance in the superconducting state. This effect is responsible for the coexistence of the nonbolometric and fast bolometric mechanisms in the normal, resistive, and superconducting states of YBaCuO epitaxial films.

Heusinger *et al.*⁸ studied NbN films in the form of multistrip structures (having a length of $140 \mu\text{m}$ and a width of $0.8 \mu\text{m}$ separated by $3.2 \mu\text{m}$ on sapphire substrates. Separate strips made of YBaCuO epitaxial films of thickness $80 \mu\text{m}$, length $800 \mu\text{m}$, and width $80 \mu\text{m}$ were placed between contact areas. Both types of superconductors in the superconducting state exhibit a bipolar response to pulsed (100 fs) optical radiation with a wavelength of $0.8 \mu\text{m}$ and a pulse repetition frequency up to 82 MHz. The positive peak of the response for NbN had the rise and fall time ~ 40 ps and preserved its duration in the entire temperature range $20 \text{ K} < T < T_c$. It was followed by a negative peak with a fall time ~ 190 ps, which broadened with increasing temperature. According to Heusinger *et al.*⁸ this peak reflects relaxation processes in the film. For all values of bias current I_b (up to 0.3 mA) and integral power density P_1 (up to $0.6 \text{ mJ}/\text{cm}^2$), the

photoresponse preserved its shape, and its amplitude was proportional to I_b and P_1 . For YBaCuO samples, the duration of the positive and negative peaks of the response was ~ 25 ps and ~ 35 ps, respectively. The amplitude of the response on the whole was proportional to the bias current. At the same time, the response in the superconducting transition region was formed by a bi-exponential unipolar voltage peak which is correctly described in the two-temperature model.⁷¹ According to Semenov *et al.*,⁷¹ the mechanism of the response away of the transition is associated with nonequilibrium change in the kinetic inductance of the superconductor under radiation, while the shape and amplitude of the response are determined by the temperature evolution of the number density of Cooper pairs. This is confirmed by good agreement between experimental results and the theory developed in Ref. 71, which gives a relation between the response voltage and the change dN_{sc} in the number density of pairs under irradiation. It is assumed that the working temperature should be maintained below T_c (away from the transition temperature) to optimize the speed of response of a detector based on the given effect since the signal has no slow "tail" characteristic of the resistive state at low temperatures.

Salient features and conditions for realization of the mechanism

- (1) Depending on temperature, the response is almost constant at low temperatures and decreases abruptly as T_c is approached.
- (2) The response associated with the breaking of Cooper pairs appears at lower threshold levels of the signal as compared to the bolometric component, has much higher speed (10–100 ps), and is characterized by clearly manifested saturation as a function of radiation intensity.
- (3) The temperature dependence of the response at low temperatures is either exponential, or coincides with the temperature dependence of critical current (for $h\nu > 2\Delta$ and for large deviations from equilibrium).
- (4) The amplitude of the response increases sharply with the bias current (more steeply than linear dependence) and attains saturation for large I_b .

2.6. Electron heating

The idea of a bolometer based of the effect of electron heating in superconductors was put forth for the first time at the beginning of eighties by Gershenzon *et al.*⁷⁶ These authors divide all nonequilibrium effects into two large categories: Josephson and electronic detection mechanisms (JDM and EDM). The idea lies in electron heating by radiation with phonons as a thermostat. Such a mechanism can exist when the heat capacity of the phonon subsystem is higher than that of the electron subsystem: $C_{ph}/C_e > 100$.⁷⁶ The EDM was realized in practice only in two cases.⁷⁷ In one case, it was associated with granular BaPbBiO films at $T \ll T_c$ ($T_c = 13.6$ K). The radiation suppresses the order parameter in granules, which is accompanied by a decrease in the critical current of intergranular weak links and the emergence of additional resistance in the resistive state of weak links.⁶⁸ The search for this mechanism in HTSC materials

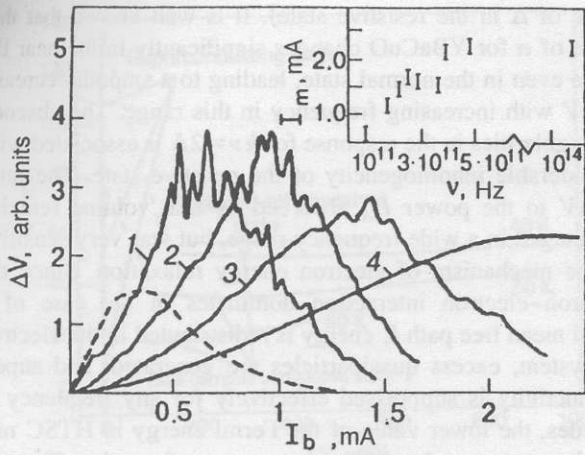


FIG. 18. Dependence of the response ΔV on the bias current I_b for a YBaCuO film for various radiation wavelengths Λ , mm: 2.2 (curve 1), 1.5 (curve 2), 1.1 (curve 3), 0.6 and 8×10^{-4} (curve 4) and $B=0$ (solid curves) and 3 T (dashed curves), $T=4.2$ K. The inset shows the frequency dependence of the maximum response current I_m (from Aksaev *et al.*⁷⁷).

did not lead to any positive results by the beginning of the nineties.⁷⁷ Another method of realization of EDM was investigated in detail for thin homogeneous Nb, Al, and NbN films.⁷⁶ The main difference between these results and those obtained in Refs. 68 is that superconductivity is suppressed considerably in the entire volume of the film, and the resistive state is attained due to transport current and/or magnetic field. The high concentration of quasiparticles as well as their small mean free path (due to scattering by defects) enhance the Coulomb interaction between quasiparticles. The latter is responsible for a lack of selectivity (absence of frequency dependence) of the heating mechanism. Indeed, high-intensity electron–electron interaction leads to an effective redistribution of absorbed energy in the electron subsystem, which is enhanced owing to secondary breaking of Cooper pairs by nonequilibrium quasiparticles and an increase in their number density. Cooling of the electron subsystem as a result of the electron–phonon interaction as well as recombination of quasiparticles turns out to be slower. The resistive state is characterized by a large steepness of dR/dT and serves as a sensitive indicator of electron heating: $\Delta V = I(dR/dT)\Delta\Theta$, where Θ is the effective electron temperature. The condition of phonon thermostat is observed for a small film thickness such that the time τ_{es} of phonon escape from the film is shorter than the time τ_{phe} of phonon–electron scattering. The time constant of the effect is determined by the electron–phonon relaxation time τ_{eph} . In a narrow range in the vicinity of the superconducting transition [$\Delta(T, H)/k_B T \ll 1$], the response relaxation time τ is associated with the dynamics of superconducting condensate and is equal to the order parameter relaxation time $\tau_\Delta \sim (k_B T/\Delta)\tau_{eph}$. A characteristic feature of electron heating is the increase in relaxation rate with temperature.

Aksaev *et al.*⁷⁷ studied bridges having a length of 0.01–4 mm and a width of 1–500 μm made of YBaCuO granular films of thickness 0.1–1 μm on Al_2O_3 and MgO substrates. All the samples under investigation could be divided into two categories: the films exhibiting typical fea-

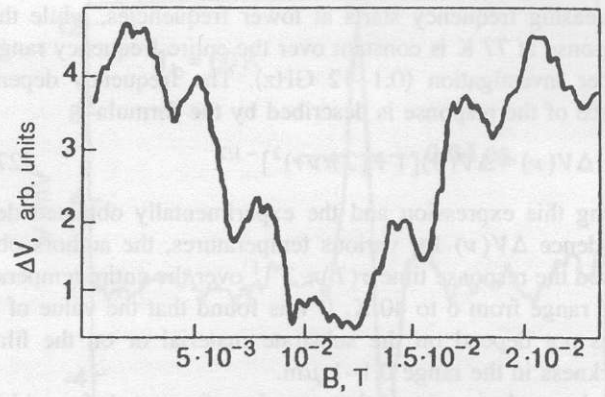


FIG. 19. Field dependence of oscillations of the response ΔV for a granular YBaCuO film at $T=4.2$ K, $\Lambda=2.2$ mm, $I=2 \mu\text{A}$ (from Aksaev *et al.*⁷⁷).

tures of JDM (A) and those in which EDM was manifested (B). The response was studied in a wide spectral range from $\Lambda=2.2$ to $8 \cdot 10^{-4}$ mm. The dependence of the response ΔV on bias current had the shape of a curve with a peak which was displaced towards higher values of I_b and became lower upon an increase in frequency. The $\Delta V(I_b)$ dependence for samples of group A had quasiperiodic peaks that “smeared” with increasing temperature, frequency, and magnetic field (Fig. 18). For radiation wavelengths $\Lambda < 0.6$ mm, the $\Delta V(I_b)$ dependences coincides (curve 4 in Fig. 18 corresponds to $\Lambda=0.6$ and $8 \cdot 10^{-4}$ mm simultaneously). Similar suppression of peaks also took place at a fixed frequency upon an increase in radiation power. A finite voltage appears on the IVC for samples belonging to both groups (A and B) for infinitely small values of $I_b \geq 0$, i.e., $I_c \approx 0$. According to Aksaev *et al.*,⁷⁷ this is due to a large spread in the parameter of weak links.

The magnetic field dependence of the response for samples of group A in the field range 10^{-2} – 10^{-3} T is oscillating with two characteristic periods $\Delta B=4 \cdot 10^{-3}$ and $1.9 \cdot 10^{-2}$ T (Fig. 19). Such oscillations are not observed for samples of group B on $\Delta V(I)$ or $\Delta V(B)$ curves.

The dependence of the response on the amplitude modulation frequency is shown schematically in Fig. 20. It can be seen that at low temperatures, the decrease in response with

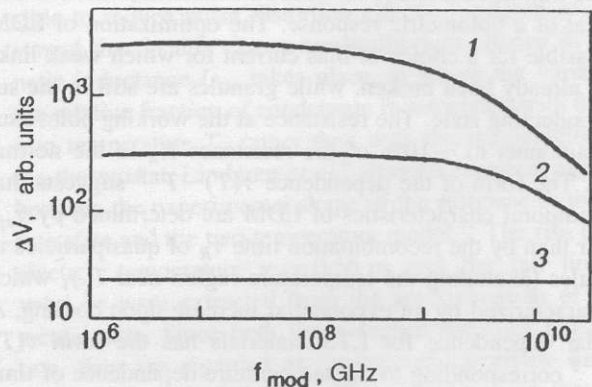


FIG. 20. Dependence of the response ΔV on the modulation frequency f_{mod} for a granular YBaCuO film with a constant impedance at various temperatures T , K: 1.7 (curve 1), 4.2 (curve 2) and 77 (curve 3) (from Aksaev *et al.*⁷⁷).